LETTERS

# Imbalance between pSmad3 and Notch induces CDK inhibitors in old muscle stem cells

Morgan E. Carlson[1], Michael Hsu[1] & Irina M. Conboy[1]

**Adult skeletal muscle robustly regenerates throughout an organism's life, but as the muscle ages, its ability to repair diminishes and eventually fails[1,2]. Previous work suggests that the regenerative potential of muscle stem cells (satellite cells) is not triggered in the old muscle because of a decline in Notch activation, and that it can be rejuvenated by forced local activation of Notch[3]. Here we report that, in addition to the loss of Notch activation, old muscle produces excessive transforming growth factor (TGF)-β (but not myostatin), which induces unusually high levels of TGF-β pSmad3 in resident satellite cells and interferes with their regenerative capacity. Importantly, endogenous Notch and pSmad3 antagonize each other in the control of satellite-cell proliferation, such that activation of Notch blocks the TGF-β-dependent upregulation of the cyclin-dependent kinase (CDK) inhibitors p15, p16, p21 and p27, whereas inhibition of Notch induces them. Furthermore, in muscle stem cells, Notch activity determines the binding of pSmad3 to the promoters of these negative regulators of cell-cycle progression. Attenuation of TGF-β/pSmad3 in old, injured muscle restores regeneration to satellite cells *in vivo*. Thus a balance between endogenous pSmad3 and active Notch controls the regenerative competence of muscle stem cells, and deregulation of this balance in the old muscle microniche interferes with regeneration.**

Satellite cells are muscle stem cells capable of lifelong maintenance and repair of myofibres, or differentiated muscle cells[4–6]. The decline in muscle tissue regeneration with age is largely due to a decreased activation of Notch pathway, which is required for satellite cells to break quiescence and prevents premature differentiation into myotubes by antagonizing Wnt pathway[3–9]. Forced activation of Notch-1, by antibody specific to its external domain (Notch-1 cleavage and activation), rejuvenates muscle repair; whereas inhibiting Notch in young muscle interferes with regeneration[3], suggesting that Notch pathway is an essential and age-specific molecular determinant of adult myogenesis.

It is widely believed that the microenvironment controls resident stem-cell behaviour[10], and our recent work established that aged muscle fibres inhibit the regenerative responses of muscle stem cells[11]. Here we examine the biochemical changes occurring in the aged microniche of muscle stem cells, for example differentiated myofibres, focusing on the age-specific interplay between active Notch and TGF-β/pSmad3 and on the ability of this signal integration to control levels of CDK inhibitors in satellite cells.

Binding of activated TGF-β proteins to their receptors induces the phosphorylation and activation of the Smad transcription factors, which form heteromers (Smad4 as a common component) that translocate into the nucleus[12–15]. Different ligands, for example TGF-β1, -β2, -β3 and myostatin, are capable of activating the same Smad2, 3 proteins[12,16,17]. Increased TGF-β signalling has been implicated in the inhibition of cell-cycle progression (both generally and in myogenic lineage), by activating CDK inhibitors and inactivating cMyc[14,18–22]. Importantly, recent genetic-targeting experiments suggest that during ageing the necessity to impose cell-cycle checkpoints becomes antagonistic to the regenerative responses of adult stem cells[23–26].

This report establishes the following causalities: (1) old myofibres inhibit their own repair by shifting balance from active Notch to over-pronounced pSmad3 in resident muscle stem cells, which upregulates p15, p16, p21 and p27 and thwarts satellite-cell regenerative capacity; (2) active Notch can override this block of satellite-cell responses by removal of pSmad3 from CDK inhibitor promoters.

Growth factors, including TGF-β family members, are typically localized and activated in a tissue's extracellular matrix (ECM), which in skeletal muscle is the main component of the basement membrane surrounding myofibres and their associated satellite cells[27].

As shown in Fig. 1, there is dramatic and constant upregulation of functional TGF-β, but not the muscle-specific family member myostatin[28], in the aged, injured and resting muscle compared with young. As expected, when present at high levels, TGF-β co-localizes with the laminin$^{+}$ basement membrane (the immediate microniche of muscle stem cells) (Fig. 1a)[29]. Isotype-matched antibody controls for these and other experiments were negative (Supplementary Fig. 1a). These data were confirmed in western blot analysis, which also established that with age both differentiated myofibres and satellite cells, located in resting and injured muscle, upregulate levels of TGF-β (inactive precursor plus bioactive protein) and pSmad3 (Fig. 1b–e and Supplementary Fig. 2). In contrast, levels of myostatin and follistatin are not changed with age (Fig. 1a–c). In agreement with previously published work[3], the levels of active Notch were reciprocal to those of pSmad3 and TGF-β, which is high in young and low in old satellite cells (Fig. 1b and Supplementary Fig. 1b). The purity of satellite cells in these preparations is greater than 95% (Supplementary Fig. 3)[3]. High levels of nuclear pSmad3 were also detected in satellite cells residing in the aged muscle *in vivo* (Supplementary Fig. 4), and excessive TGF-β was detected in old muscle at days 1 and 3 after injury (not shown).

Our recent report demonstrated that proliferation and myogenesis of even young satellite cells are inhibited by the aged myofibres[11]. Interestingly, factors secreted by aged myofibres rapidly upregulated TGF-β production by young satellite cells (Fig. 1f) in transwell co-cultures (impermeable to cell migration). This provides a molecular explanation for the pre-mature 'ageing' of young progenitor cells exposed to aged tissue.

These data establish that although both Notch and pSmad3 can be robustly activated in skeletal muscle, because their ligands are expressed by myofibres and satellite cells, with age the balance is shifted from active Notch to active TGF-β/pSmad3 (Fig. 1)[3].

During the first days after injury, satellite cells need to break quiescence and proliferate. However, there is an age-specific elevation of pSmad3 and diminished Notch activation, either one of which is

[1]Department of Bioengineering, University of California, Berkeley, California 94720, USA.

sufficient to inhibit cell-cycle progression[17,22]. We hypothesized that excessive levels of TGF-β/pSmad might upregulate the levels of CDK inhibitors in muscle stem cells, whereas activation of Notch might antagonize this process. After muscle injury, satellite cells were derived from young muscle[3] and cultured with TGF-β1, with or without simultaneous forced activation of Notch. Compared with untreated cells, exogenously added TGF-β1 caused a prompt upregulation of p15, p16, p21 and p27 in satellite cells (Fig. 2a, quantified in Fig. 2b). When endogenous Notch was experimentally activated, simultaneously with TGF-β1 treatment, the inducing effects on p15, p16, p21 and p27 levels were significantly attenuated (Fig. 2a, b and Supplementary Fig. 5c) at a range of TGF-β1 concentrations (Supplementary Fig. 5). Manipulation of TGF-β/pSmad and active Notch balance not only controls CDK inhibitor levels, but also regulates proliferation of satellite cells in their endogenous microniches (Supplementary Fig. 6).

To analyse this antagonistic interaction with higher precision, we examined whether active Notch and pSmad3 physically interact on promoters of the p15, p16, p21 and p27 genes. A pSmad3-specific chromatin immunoprecipitation assay (ChIP) was performed on satellite cells treated with TGF-β only, activation of Notch only, TGF-β and activation of Notch together or untreated.

As shown in Fig. 2c, both active Notch and RNA polymerase II are detected in a complex with pSmad3, suggesting that active Notch and pSmad3 physically interact on gene regulatory regions. Consistent with the idea of functional balance, forced activation of Notch yielded more endogenous Notch and treatment with TGF-β yielded more pSmad3 in these complexes (Fig. 2c).

DNA co-precipitated with pSmad3 was analysed by quantitative polymerase chain reaction (Q-PCR), using primers specific for 5′ promoter regulatory regions of p15, p16, p21 and p27 (Fig. 2d, e). These data provided a further understanding of the molecular mechanism of active Notch and TGF-β/pSmad3 antagonism. Namely, forced activation of Notch dramatically reduced pSmad3 presence on the promoter regions of p15, p16, p21 and p27, even in the presence of TGF-β treatment (Fig. 2d, e).

Interestingly, in the absence of Notch activation (by γ-secretase inhibitor (GSI)), young/low levels of TGF-β are sufficient to induce p15, p16, p21 and p27 proteins (Fig. 3a, b); and pSmad3 presence on the promoters of these genes increases in young muscle stem cells (Fig. 3d, e). Expectedly, less active Notch was detected in Notch–pSmad3 complexes after treatment with GSI, whereas pSmad3 levels were not affected (Fig. 3c). These results were confirmed with several sets of PCR primers spanning about 1 kilobase of the studied regulatory regions; and corroborated by negative controls, including the lack of amplification of a Smad3 non-enriched genome region (Supplementary Fig. 7).

These data show that in muscle stem cells, active Notch attenuates age-specific induction of multiple CDK inhibitors by reducing the presence of pSmad3 on their promoter regions; and that either diminished Notch activation or increased TGF-β/pSmad3 levels are sufficient for upregulating these negative regulators of cell-cycle progression (Figs 2 and 3, and Supplementary Figs 6 and 7). Interestingly, p16 is sensitive to a slight increase in pSmad3, as inhibition of Notch robustly enhanced pSmad3 binding, whereas Notch activation did not significantly reduce TGF-β imposed pSmad3 binding to the p16 promoter (Figs 2, 3 and Supplementary Fig. 7).

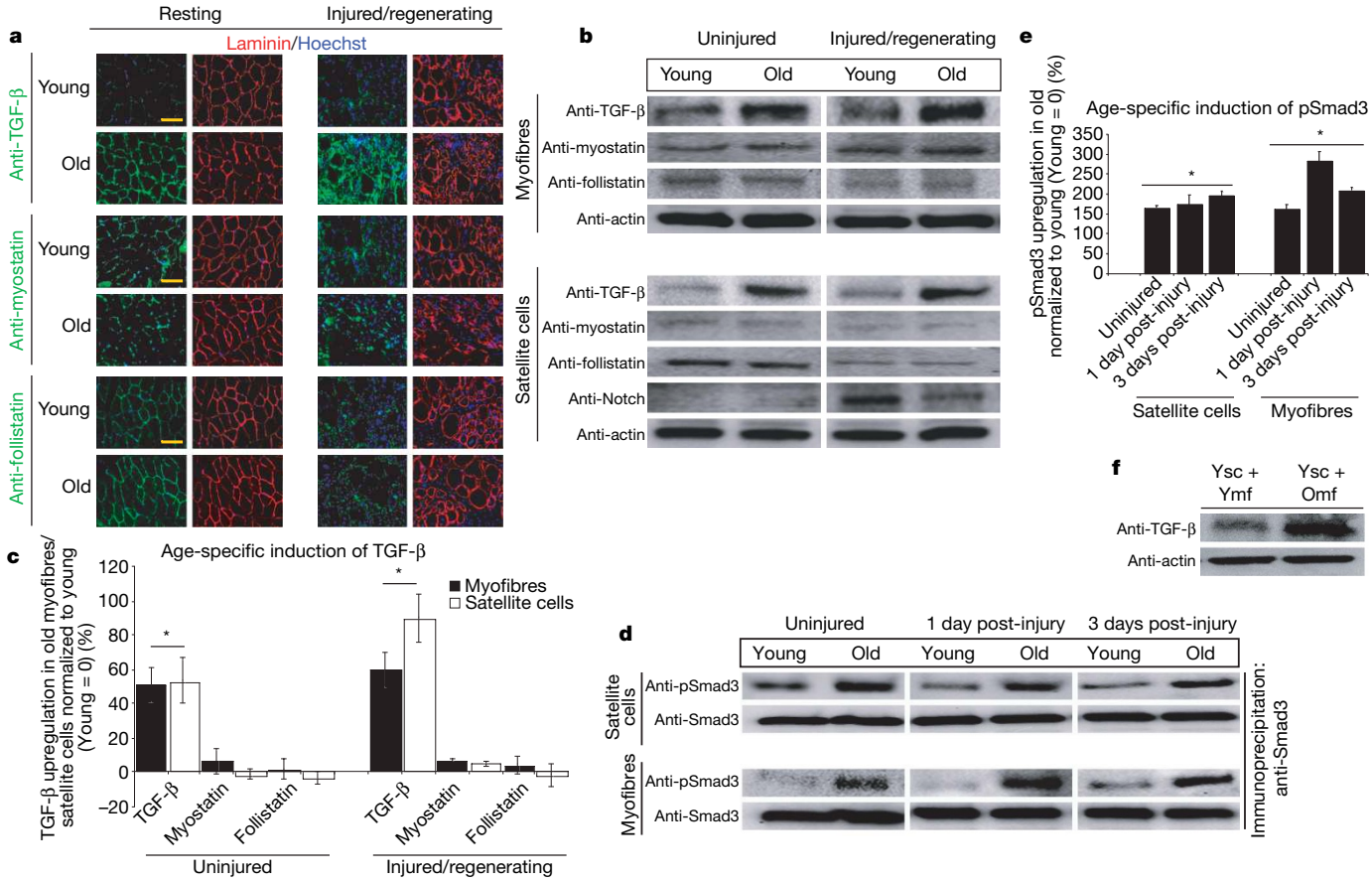


**Figure 1 | TGF-β/pSmad3, but not myostatin, increases in old skeletal muscle.** **a**, Immunodetection of TGF-β, myostatin or follistatin (green) and laminin (red) in 10-μm skeletal muscle cryosections. Hoechst labels nuclei (blue). Scale bar, 50 μm. **b**, Western blot on myofibres and satellite cells; quantified in **c**. **d**, Immunoprecipitation with anti-Smad3 antibody, followed by western blot with anti-phosphorylated Smad3 antibody; quantified in **e**. **f**, After overnight transwell co-culture with young or old myofibres, young satellite cells were analysed by western blotting; data are means ± s.d., $n = 3$. *$P \leq 0.05$ compared with young.

To confirm these findings and address their physiological significance *in vivo*, we examined whether aged muscle stem cells would effectively repair old tissue when pSmad3 is locally attenuated by lentivirally delivered short hairpin RNA (shRNA) to *Smad3*.

Young and old muscles were infected with the following lentiviral particles *in vivo*: three different *Smad3*-targeted shRNAs, non-target shRNA to control for non-specific RNA interference or transduction control; and followed by muscle injury (Fig. 4 and Supplementary Figs 8–10). As expected, at 5 days after injury, old control muscle contains fewer regenerated myofibres than young, based on haematoxylin and eosin histology and immunodetection of eMyHC *de novo* myofibres with centrally located bromodeoxyuridine ($BrdU^+$) nuclei that are the fusion product of myoblasts generated by satellite cells (Fig. 4)[3]. In contrast to control viral transduction and non-target shRNA control, the acute *in vivo* expression of each one of the *Smad3*-targeted shRNAs enhanced and rejuvenated regeneration of old muscle (Fig. 4a, b and Supplementary Fig. 10a). Furthermore, in old muscle satellite cells there was pronounced increase in p15 (at all times) and p21 (upon muscle injury); and importantly, p15 and p21 were attenuated *in vivo* to their 'youthful' levels by each tested *Smad3*-targeted shRNA, but not by non-target shRNA (Fig. 4c, d). The levels of p16 and of p21, p27 were not increased in quiescent satellite cells endogenous to old resting muscle, consistent with rapid activation of their myogenic responses in young environments (Fig. 4c, d)[3,11]. A slight increase in p16 and p27 levels was detected 24 h after injury, suggesting a potential physiological importance for early muscle stem-cell responses (Supplementary Fig. 9). Thus, elevated TGF-β/pSmad3 assures the age-dependent upregulation of at least one CDK inhibitor at all times, while specific time points are expectedly different for individual CDK inhibitors known to be under control of many molecular cues. These data strongly suggest that Smad3-specific (rather than non-target effects[30]) rescued the satellite-cell regenerative responses in old niches, as three different *Smad3*-targeted shRNAs similarly enhanced myogenesis of old muscle and diminished the levels of p15 and p21, but not of p16 and p27 in the aged satellite cells (Fig. 4a–d and Supplementary Fig. 10). *Smad3* targeting of these shRNAs is confirmed by the expected downregulation of messenger RNA levels of *Smad3* and nuclear levels of pSmad3 protein, as well as of Smad3, Smad6, Smad7, TGF-β and myostatin in satellite cells *in vivo*[14,15] (Supplementary Fig. 10b–e). Notably, pan-neutralizing antibody against TGF-β rejuvenated repair of old muscle, and recombinant TGF-β resulted in scarring of young muscle (Supplementary Fig. 11), both of which are consistent with the effects of Smad3 targeting by three different shRNAs.

In contrast, inhibition of myostatin by follistatin resulted in multitudes of very small nascent myofibres, and proliferating $Myf\text{-}5^+$ myogenic cells that persisted within the injured area (Supplementary Fig. 11). Such a defect in myogenic differentiation was also evident when both TGF-β and myostatin were neutralized; strongly suggesting that myostatin, which remains constant with age (Fig. 1), is required for productive differentiation of myogenic cells into myofibres. Distinct regenerative outcomes, where neutralization of TGF-β but not myostatin restores productive repair to old muscle, confirms that TGF-β is the main age-specific local inhibitor in skeletal muscle niche.

Comprehensively, this work establishes that productive muscle repair is determined by an antagonistic balance between the levels of TGF-β/pSmad3 (low in young and high in old) and the activation of Notch (high in young and low in old)[3], which regulates the levels of four distinct CDK inhibitors in resident stem cells. An age-specific shift in either pathway would suffice for the upregulation of CDK inhibitors and diminished proliferation of muscle stem cells. Deregulation of both Notch and TGF-β/pSmad3 thus assures the lack of satellite-cell activation in the context of aged microniche.

Our data indicate that TGF-β does not directly inhibit the expression of Notch ligand Delta, or the levels of active Notch in satellite cells (Supplementary Fig. 12). Likewise, activation of Notch does not directly diminish the TGF-β/pSmad3 levels (Figs 2 and 3). Hence, the

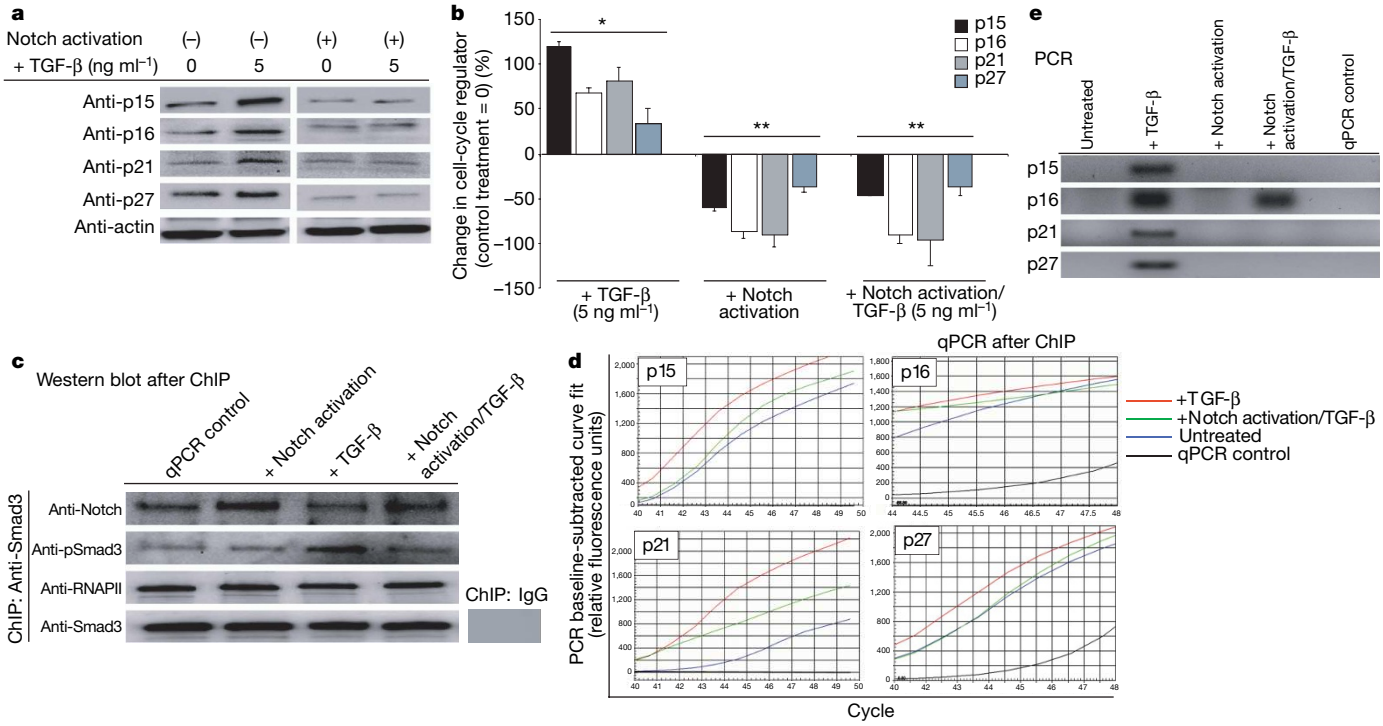


**Figure 2 | Notch removes pSmad3 from the 5′ regulatory regions of CDK inhibitors.** **a**, Satellite cells treated with TGF-β1, with or without Notch activation, were analysed by western blotting for p15, p16, p21 and p27; quantified in **b**. $*P \leq 0.05$ compared with untreated control (0); $**P \leq 0.05$ compared with TGF-β. Smad3 co-precipitated proteins (**c**) were resolved by western blot; genomic DNA (**d**) was analysed by RT–qPCR, using primers specific for 5′ regions of CDK inhibitors; data are means ± s.d., $n = 3$. **e**, qPCR reactions after 44 cycles revealed fragments of expected molecular weight on agarose gel.

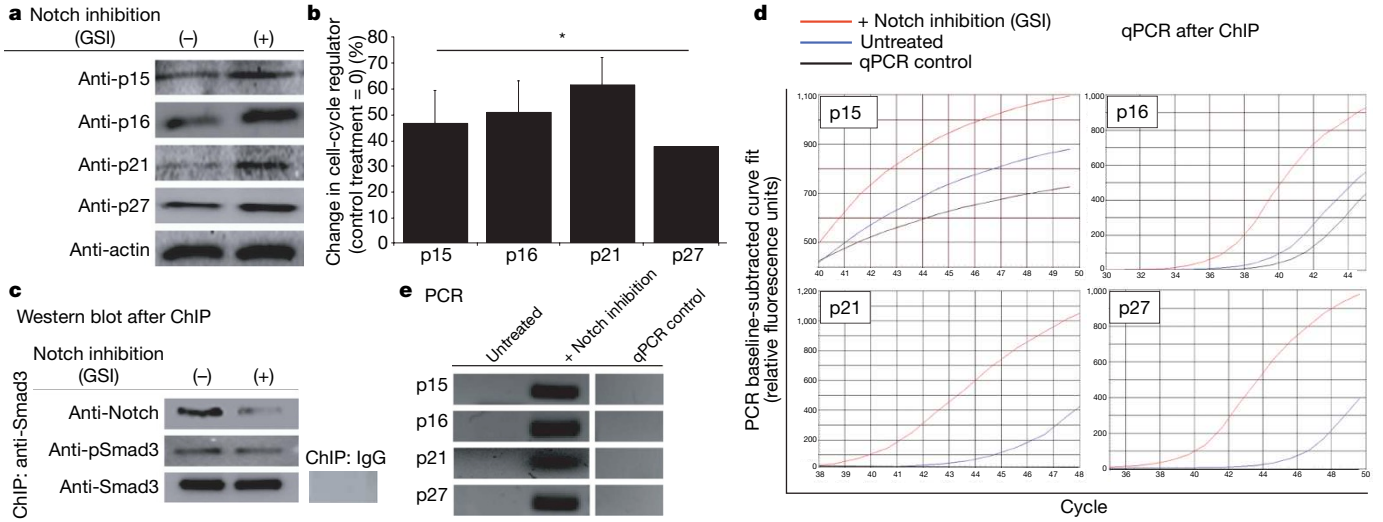


**Figure 3 | Inhibition of endogenous Notch upregulates CDK inhibitors.** **a**, Compared with untreated cells (−), Notch inhibition by GSI caused prompt upregulation of p15, p16, p21 and p27; western blot assays quantified in **b**; $*P \leq 0.05$ compared with untreated control. In ChIP assay, Smad3 co-precipitated proteins were resolved by western blot (**c**), genomic DNA (**d**) was analysed by RT–qPCR, using primers to p15, p16, p21 and p27 5′ regulatory regions; data are means ± s.d., $n = 3$. **e**, qPCR reactions after 44 cycles revealed fragments of expected molecular weight on agarose gel.

age-specific changes in reciprocal activation of Notch and TGF-β/pSmad3 seem to initiate independently of each other, and future work will identify molecular triggers causing such imbalance. Additional studies will also answer whether excessive TGF-β found in old muscle ECM reflects only local secretion or also results from higher levels of TGF-β in the aged circulation, and whether local and systemic TGF-β are connected and provide feedbacks for each other. Importantly, this work has established that one factor in the ageing of

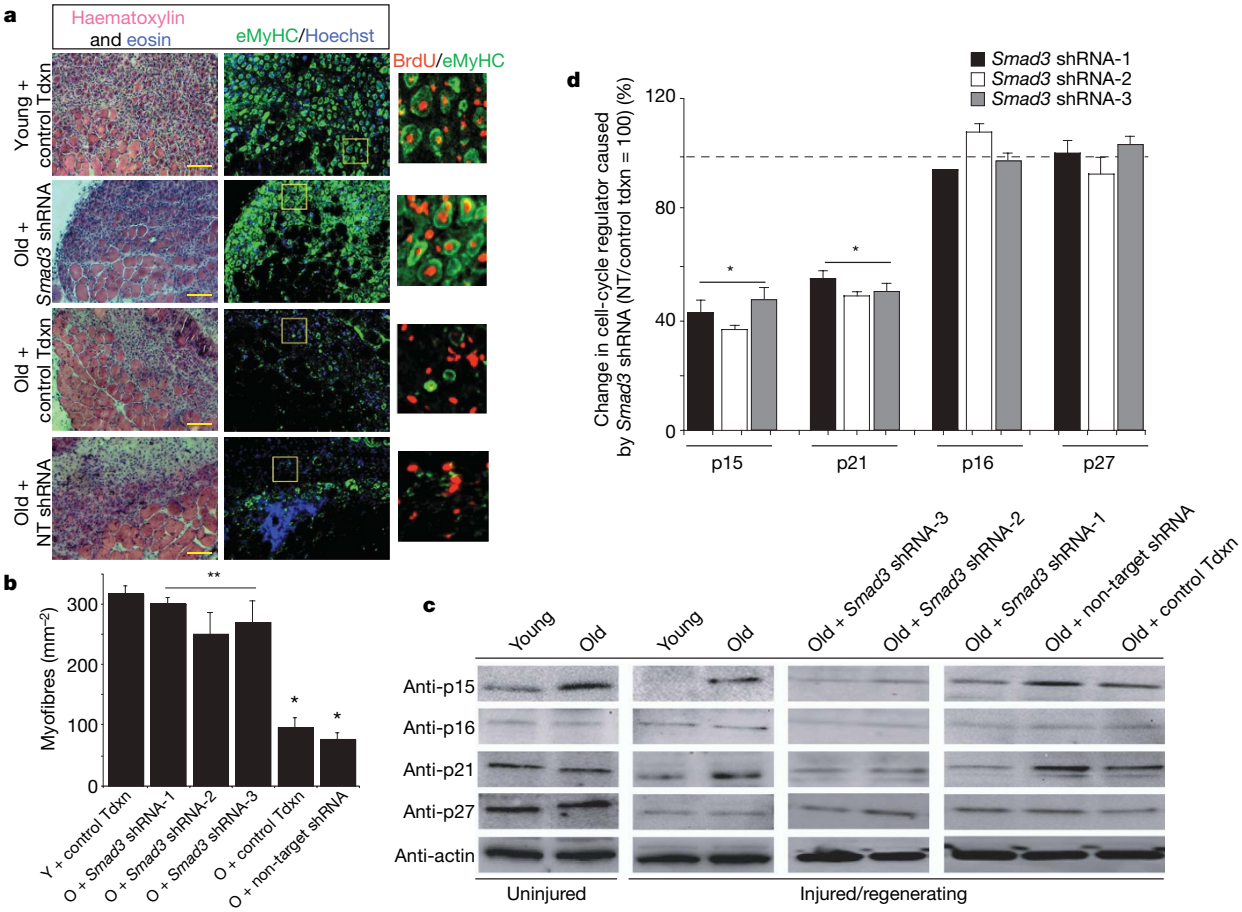


**Figure 4 | *Smad3* shRNA rescues responses of satellite cells in old niche *in vivo*.** Lentiviral-infected muscle (control transduction (Tdxn), *Smad3* shRNAs, non-target shRNA) was analysed 5 days after injury. **a**, Haematoxylin and eosin 10-μm cryosections of *Smad3* shRNA-1; quantified in **b**; $n = 15$, *, $**P \leq 0.05$; individual *Smad3* shRNA-2, -3 data in Supplementary Fig. 10a; immunodetection of eMyHC myofibres with $BrdU^+$ nuclei. Scale bar, 100 μm; O, old; Y, young. **c**, Isolated satellite cells analysed by western blot for p15, p16, p21 and p27; quantified in **d**; $*P \leq 0.05$, compared with non-target shRNA, control tdxn; data are means ± s.d., $n = 3$.

skeletal muscle—and perhaps other organ niches—seems to be a self-imposed inhibition of regenerative potential.

## METHODS SUMMARY

Young (~2 month) and old (~24 month) C57 BL/6 mice were from Jackson Laboratories and the National Institute on Ageing. Skeletal muscle was cardiotoxin injured[3]. Co-injection with anti-TGF-β neutralizing antibody, TGF-β, follistatin or IgG was performed in some experiments. Muscle was isolated 1–5 days after injury and prepared for cryosectioning/histology, western blotting or *in vitro* culturing of myofibre explants and satellite cells.

Immunocytochemistry/histological analyses were performed as described[3,11]. Samples were analysed with a Zeiss Axio Imager A1, imaged with an Axiocam MRc camera and AxioVision software. Western blots were analysed with Bio-Rad Gel Doc/Chemi Doc Imaging System and Quantity One software.

Transwell co-cultures (1 μm) were performed with isolated satellite cells and young/old myofibres. Conditioned supernatants were analysed for secreted bioactive TGF-β1 levels in enzyme-linked immunosorbent assay (ELISA)-based cytokine antibody arrays (Raybiotech). CDK inhibitors were induced *in vitro* by culturing isolated satellite cells with TGF-β1 or myostatin. Notch was activated by immobilized Delta or EDTA exposure before seeding.

Lentiviral transduction was performed with distinct *Smad3* shRNAs: accession number NM_016769.2. (shRNA-2): CCGGCCTTACCACTATCAGAGA GTACTCGAGTACTCTCTGATAGTGGTAAGGTTTTTG, (shRNA-3)-CCGG CTGTCCAATGTCAACCGGAATCTCGAGATTCCGGTTGACATTGGACAG-TTTTTG. *Smad3* shRNA cocktail (shRNA-1, see Methods) yielded results similar to shRNAs 2, 3. Control transduction with non-target shRNA or GFP transduction lentiviral particles was also performed.

BrdU was injected intraperitoneally, 3 days after injury. Tissues were analysed 5 days after injury for regenerative responses and transduction levels by histological analysis, western blotting and PCR with reverse transcription (RT–PCR) (Bio-Rad iQ5).

In ChIP assays (Upstate), satellite cells underwent treatments for 24 h, followed by DNA shearing and immunoprecipitations. Proteins co-precipitated with pSmad3 were analysed by western blot. pSmad3 co-precipitated DNA was analysed using primers to the gene regulatory regions of p15, p16, p21 and p27. Real-time qPCR samples were analysed using a Bio-Rad iQ5 real-time PCR detection system, with iQ5 optical system software. Standard PCR samples were analysed with a Bio-Rad iQ5 thermal cycler.

**Full Methods** and any associated references are available in the online version of the paper at www.nature.com/nature.

**Received 6 November 2007; accepted 28 April 2008.**
**Published online 15 June 2008.**

1. Grounds, M. D. Age-associated changes in the response of skeletal muscle cells to exercise and regeneration. *Ann. NY Acad. Sci.* **854,** 78–91 (1998).
2. Renault, V., Thornell, L. E., Eriksson, P. O., Butler-Browne, G. & Mouly, V. Regenerative potential of human skeletal muscle during aging. *Aging Cell* **1,** 132–139 (2002).
3. Conboy, I. M., Conboy, M. J., Smythe, G. M. & Rando, T. A. Notch-mediated restoration of regenerative potential to aged muscle. *Science* **302,** 1575–1577 (2003).
4. Wagers, A. J. & Conboy, I. M. Cellular and molecular signatures of muscle regeneration: current concepts and controversies in adult myogenesis. *Cell* **122,** 659–667 (2005).
5. Collins, C. A. & Partridge, T. A. Self-renewal of the adult skeletal muscle satellite cell. *Cell Cycle* **4,** 1338–1341 (2005).
6. Morgan, J. E. *et al.* Myogenic cell proliferation and generation of a reversible tumorigenic phenotype are triggered by preirradiation of the recipient site. *J. Cell Biol.* **157,** 693–702 (2002).
7. Schultz, E. & Lipton, B. H. Skeletal muscle satellite cells: changes in proliferation potential as a function of age. *Mech. Ageing Dev.* **20,** 377–383 (1982).
8. Brack, A. S. *et al.* Increased Wnt signaling during aging alters muscle stem cell fate and increases fibrosis. *Science* **317,** 807–810 (2007).
9. Conboy, I. M. *et al.* Rejuvenation of aged progenitor cells by exposure to a young systemic environment. *Nature* **433,** 760–764 (2005).
10. Li, L. & Xie, T. Stem cell niche: structure and function. *Annu. Rev. Cell Dev. Biol.* **21,** 605–631 (2005).
11. Carlson, M. E. & Conboy, I. M. Loss of stem cell regenerative capacity within aged niches. *Aging Cell,* (2007).
12. Massague, J. TGF-beta signal transduction. *Annu. Rev. Biochem.* **67,** 753–791 (1998).
13. Massague, J. & Chen, Y. G. Controlling TGF-beta signaling. *Genes Dev.* **14,** 627–644 (2000).
14. Derynck, R. & Zhang, Y. E. Smad-dependent and Smad-independent pathways in TGF-beta family signalling. *Nature* **425,** 577–584 (2003).
15. Feng, X. H. & Derynck, R. Specificity and versatility in tgf-beta signaling through Smads. *Annu. Rev. Cell Dev. Biol.* **21,** 659–693 (2005).
16. Natarajan, E. *et al.* A keratinocyte hypermotility/growth-arrest response involving laminin 5 and p16INK4A activated in wound healing and senescence. *Am. J. Pathol.* **168,** 1821–1837 (2006).
17. Ito, T., Sawada, R., Fujiwara, Y., Seyama, Y. & Tsuchiya, T. FGF-2 suppresses cellular senescence of human mesenchymal stem cells by down-regulation of TGF-beta2. *Biochem. Biophys. Res. Commun.* **359,** 108–114 (2007).
18. Untergasser, G. *et al.* Profiling molecular targets of TGF-beta1 in prostate fibroblast-to-myofibroblast transdifferentiation. *Mech. Ageing Dev.* **126,** 59–69 (2005).
19. Olson, N. E., Kozlowski, J. & Reidy, M. A. Proliferation of intimal smooth muscle cells. Attenuation of basic fibroblast growth factor 2-stimulated proliferation is associated with increased expression of cell cycle inhibitors. *J. Biol. Chem.* **275,** 11270–11277 (2000).
20. Joulia, D. *et al.* Mechanisms involved in the inhibition of myoblast proliferation and differentiation by myostatin. *Exp. Cell Res.* **286,** 263–275 (2003).
21. Lin, J. *et al.* P27 knockout mice: reduced myostatin in muscle and altered adipogenesis. *Biochem. Biophys. Res. Commun.* **300,** 938–942 (2003).
22. Rao, P. & Kadesch, T. The intracellular form of notch blocks transforming growth factor beta-mediated growth arrest in Mv1Lu epithelial cells. *Mol. Cell. Biol.* **23,** 6694–6701 (2003).
23. Janzen, V. *et al.* Stem-cell ageing modified by the cyclin-dependent kinase inhibitor p16INK4a. *Nature* **443,** 421–426 (2006).
24. Molofsky, A. V. *et al.* Increasing p16INK4a expression decreases forebrain progenitors and neurogenesis during ageing. *Nature* **443,** 448–452 (2006).
25. Krishnamurthy, J. *et al.* p16INK4a induces an age-dependent decline in islet regenerative potential. *Nature* **443,** 453–457 (2006).
26. Stepanova, L. & Sorrentino, B. P. A limited role for p16Ink4a and p19Arf in the loss of hematopoietic stem cells during proliferative stress. *Blood* **106,** 827–832 (2005).
27. Husmann, I., Soulet, L., Gautron, J., Martelly, I. & Barritault, D. Growth factors in skeletal muscle regeneration. *Cytokine Growth Factor Rev.* **7,** 249–258 (1996).
28. McPherron, A. C., Lawler, A. M. & Lee, S. J. Regulation of skeletal muscle mass in mice by a new TGF-beta superfamily member. *Nature* **387,** 83–90 (1997).
29. Barcellos-Hoff, M. H. Latency and activation in the control of TGF-beta. *J. Mammary Gland Biol. Neoplasia* **1,** 353–363 (1996).
30. Svoboda, P. Off-targeting and other non-specific effects of RNAi experiments in mammalian cells. *Curr. Opin. Mol. Ther.* **3,** 248–257 (2007).

**Supplementary Information** is linked to the online version of the paper at www.nature.com/nature.

**Acknowledgements** We thank R. Derynck and M. Conboy for discussions. This work was supported by National Institutes of Health (NIH) R01 (AG027252), NIH R21 (AG27892) and Ellison's Medical Foundation grants to I.M.C., and a Pre-doctoral Training Fellowship from the California Institute for Regenerative Medicine training grant to M.E.C.

**Author Contributions** M.E.C. performed all experiments, analysed the data and contributed to the writing of the manuscript; M.H. performed preliminary experiments for Fig.1a, b, d and Supplementary Figs 4 and 11; and I.M.C. designed the study, participated in experiments, interpreted the data and wrote the manuscript.

**Author Information** Reprints and permissions information is available at www.nature.com/reprints. Correspondence and requests for materials should be addressed to I.M.C. (iconboy@berkeley.edu).

## METHODS

**Animal strains.** Young (2–3 month) and old (22–24 month) C57 BL/6 male mice were obtained from pathogen-free breeding colonies at Jackson Laboratories and the National Institute on Ageing, respectively. Animals were housed at the Northwest Animal Facility, University of California, Berkeley. Animal procedures were conducted in accordance with the Administrative Panel on Laboratory Animal Care at University of California, Berkeley.

**Muscle injury.** Tibialis anterior and gastrocnemius muscles of mice were injected with 5 ng cardiotoxin (CTX-1) (Sigma), suspended in 1 × PBS at four or five sites in each muscle (10 μl per site), using a 28-gauge needle. In some experiments anti-TGF-β neutralizing antibody, TGF-β or control goat IgG (all at 500 ng ml$^{-1}$ final concentration) were co-injected with CTX-1, following the same protocol as described above for CTX alone. Uninjured or injured/regenerating muscle tissue was isolated 1–5 days after injury. Whole muscle was prepared for cryosectioning and histological analysis, western blotting or for use in culturing of isolated satellite cells *in vitro*.

**Muscle isolation and satellite-cell culture.** Myofibre explants and satellite cells were generated from C57 BL/6 mice as described previously[3,11]. Briefly, whole muscle underwent enzymatic digestion at 37 °C in DMEM (Invitrogen)/1% penicillin–streptomycin (Invitrogen)/125 U ml$^{-1}$ Collagenase Type IIA (Sigma) solution. Bulk myofibres with associated satellite cells (located beneath the basement membrane and above the plasma membrane) were purified away from muscle interstitial cells, tendons, etc. by multiple rounds of trituration, sedimentation and washing. Satellite cells were isolated from purified myofibres by subsequent enzymatic digestion with Collagenase Type IIA and Dispase (Sigma), followed by sedimentation, washing and fine-mesh straining procedures, as in refs 3 and 11. Purified satellite cells and satellite cell-stripped myofibres were used in subsequent experiments, as described below. The approximate 95% purity of satellite cells was routinely confirmed by generation of proliferating fusion-competent myoblasts after 24 h in growth medium (Ham's F-10 (Mediatech), 20% FBS (Mediatech), 5 ng ml$^{-1}$ FGF (Chemicon) and 1% penicillin–streptomycin); and myotube formation after 48 h in DMEM, +2% horse serum. The efficiency of satellite-cell depletion from myofibres was routinely confirmed by the absence of such myogenic potential. Satellite cells were cultured on ECM:PBS-coated plates (1:500; BD Biosciences).

**Transwell co-cultures of myofibres and satellite cells.** Transwell co-cultures (1.0 μm, Corning) were used for culturing isolated satellite cells with young or old myofibres. Satellite cells were seeded onto ECM-coated plates in OPTI-MEM (Invitrogen), +5% FBS. Transwell inserts, containing isolated myofibre explants from young or old muscle, were placed over satellite cells and cultured for 72–96 h before lysing for western blot analysis (see below). Supernatants conditioned for 24 h, from both young and old control myofibre explants, were used to analyse secreted bioactive TGF-β1 levels (immunodetection of active protein) in ELISA-based cytokine antibody arrays (RayBiotech).

**Western blot analysis.** Myofibre and satellite-cell lysates were prepared in lysis buffer (50 mM Tris, 150 mM NaCl, 1% NP40, 0.25% sodium deoxycholate and 1 mM EDTA, pH 7.4). Protease inhibitor cocktail (Sigma) and 1 mM PMSF were added before use. Phosphatase activity was inhibited by 1 mM sodium fluoride and 1 mM sodium orthovanadate for pSmad immunodetection. Approximately 30 μg protein extract were run on pre-cast SDS PAGE gels (Biorad). Primary antibodies were diluted in 5% non-fat milk/1 × PBST, and nitrocellulose membranes were incubated with antibody mixtures overnight at 4 °C. HRP-conjugated secondary antibodies (Santa Cruz Biotech) were diluted 1:1,000 in 1 × PBST/1% BSA and incubated for 1 h at room temperature. Blots were developed using Western Lightning ECL reagent (Perkin Elmer), and analysed with Bio-Rad Gel Doc/Chemi Doc Imaging System and Quantity One software. Results of multiple assays were quantified by digitizing the data and normalizing pixel density of examined protein by actin-specific pixel density.

**Immunocytochemistry and histological analysis.** Muscle tissue was treated in a 25% sucrose/PBS solution, frozen in OCT compound (Tissue Tek), cryosectioned at 10 μm (Thermo Shandon Cryotome E) and immunostained as previously described[3,11]. Immunostaining or haematoxylin and eosin staining were performed on cryosections. For indirect immunoflourescence, sections were permeabilized in (PBS, +1% FBS, +0.25% Triton X-100), incubated with primary antibodies for 1 h at room temperature in PBS, +1%FBS, and then with fluorophore-conjugated, species-specific secondary antibodies for 1 h at room temperature (1:500 in PBS, +1%FBS). pSmad3- and BrdU-specific immunostaining required additional nuclear permeabilization and DNA-chromatin denaturation with 4 N HCL. Nuclei were visualized by Hoechst staining for all immunostains. Biologically active TGF-β and myostatin proteins (immunodetectible ligands cleaved from the latent complex)[14,29] were also examined. Samples were analysed at room temperature with a Zeiss Axio Imager A1, and imaged with an Axiocam MRc camera and AxioVision software.

***In vitro* induction of cell-cycle regulators by TGF-β and myostatin.** Activated-by-injury satellite cells were isolated from injured muscle. Cells were seeded onto ECM-coated, six-well plates at a uniform density of $1.2 \times 10^5$ cells per well, and cultured for 24 h in OPTI-MEM +1% mouse sera, containing various levels of TGF-β1 or myostatin. For Notch activation, ECM-coated plates were coated with 2 μg ml$^{-1}$ Delta-4 (DLL4) overnight at 37 °C, before seeding satellite cells. Alternatively, Notch activation was induced by exposing satellite cells to 5 mM EDTA for 15 min at 37 °C before seeding. Cells lysates were prepared and used for western blotting analysis (described above).

**shRNA delivery by lentiviral transduction.** Young and old tibialis anterior and gastrocnemius muscles were infected, *in vivo*, with control non-target shRNA (Sigma SHC002V), GFP (Sigma SHC003V) or pLKO.1-puro (Sigma SHC001V) control transduction lentiviral particles (at least $10^6$ transducing units per millilitre, as determined by p24 antigen ELISA titre). Mouse *Smad3* shRNA-producing lentiviral particles (also obtained from Sigma) were used for *in vivo* transduction experiments (target-set generated from accession number NM_016769.2: (1) CCGGCCCATGTTTCTGCATGGATTTCTCGAGAAATCC ATGCAGAAACATGGGTTTTTG; (2) CCGGCCTTACCACTATCAGAGAGTA CTCGAGTACTCTCTGATAGTGGTAAGGTTTTTG; (3) CCGGCTGTCCAA TGTCAACCGGAATCTCGAGATTCCGGTTGACATTGGACAGTTTTTG; (4) CCGGGCACACAATAACTTGGACCTACTCGAGTAGGTCCAAGTTATTGT-GTGCTTTTTG; (5) CCGGCATCCGTATGAGCTTCGTCAACTCGAGTTGAC GAAGCTCATACGGATGTTTTTG). shRNAs were used in a *Smad3* shRNA cocktail (shRNAs 1–5), designated *Smad3* shRNA-1, or individually (shRNA(2) designated *Smad3* shRNA-2 and shRNA(3) designated *Smad3* shRNA-3). Skeletal muscle was infected by intramuscular injection of lentiviral particles (about 50,000 TU) with a 28-gauge needle on multiple consecutive days, before or coincident with CTX-1 injury. To examine cell proliferation, 50 μl of 10 mM BrdU was injected intraperitoneally at 3 days after injury. Tissues were analysed for regenerative responses and transduction levels at 5 days after injury by cryo-sectioning of whole tissues, or western blotting of satellite-cell lysates (described above). Transcript levels were analysed using SuperScript RT–PCR kit (Invitrogen) for amplification of Smad3 (F = CTGGCTACCTGAGTGAAGATGGAGA, R = AAAGACCTCCCCTCCG ATGTAGTAG) and GAPDH (F = TGAGGCCGGTGCTGAGTATGTCGTG, R = TCCTTGGAGGCCATGTAGGCCAT). Amplification products (25–40 cycles on BioRad iQ5) were examined and confirmed for predicted molecular masses on EtBr-stained 2% agarose gels.

**ChIP assays and RT–qPCR/PCR.** Isolated satellite cells were treated with TGF-β1 only, activation of Notch only, TGF-β1/Notch together, Notch inhibition (GSI) or untreated (as described above). After culture for 24 h, satellite cells were fixed with 1% PFA and ChIP assay was performed according to manufacturer's guidelines (Upstate). Fragments of about 500 base pairs were produced by shearing DNA with attached proteins (confirmed by EtBr-stained gels), and precipitated with antibodies to DNA-bound protein. Proteins that co-precipitated with pSmad3 were analysed by western blot, using indicated antibodies. DNA that co-precipitated with pSmad3 was analysed using primers specific for the 5′ gene regulatory regions of p15, p16, p21 and p27 (p15 F = TCACCGAAGCTACTGGGTCT , R = GTTCAGGGCGTTGGGATCT; p16 F = GTCACACGACTGGGCGATT, R = GTTGCCCATCATCATCACCT and F = GATGACTTCACCCCGTCACT, R = AACACCCCTGAAAACACTGC/GT CCCTCCTTCCTTCCTCTG; p21 F = CCGCGGTGTCAGAGTCTA, R = CAT GAGCGCATCGCAATC; p27 F = AGCCTACGCTCCGACTGTT, R = AGTT CTGCGACTGCACACAG and F = CTAGCCACCGAAGCTCCTAA, R = AGT TCTGCGACTGCACACAG and F = CTGGCTCTGCTCCATTTGAC, R = G GCTCCCGTTAGACACTCTC). GAPDH primers (see above) were used as control for Smad3 non-enriched genomic regions. Primers were designed with OligoPerfect Designer (Invitrogen). For RT–qPCR, samples were analysed using a Bio-Rad iQ5 real-time PCR detection system, with iQ5 optical system software. For PCR, samples were amplified with Platinum Taq DNA Polymerase (Invitrogen) and analysed on a Bio-Rad iQ5 system. After 40–55 cycles of amplification, fragments produced from each primer set were examined and confirmed for their predicted molecular masses on EtBr-stained 2% agarose gels. Fifty-five cycles of amplification were used for negative control PCR reactions.

**Reagents.** Antibodies to BrdU (ab6326), activated Notch1 (ab8925) and CHiP grade Smad3 (ab287379) were purchased from Abcam. Antibody to developmental eMyHC (clone RNMy2/9D2) was acquired from Vector Laboratories. Antibodies to desmin (clone DE-U-10, Cat#D8281), laminin (L9393), actin (A5060) and follistatin (F2177) were acquired from Sigma. Bioactivity-neutralizing antibodies against TGF-β1/2/3 were obtained from R&D Systems (MAB1835) and Santa Cruz Biotechnologies (sc7892). Antibodies to myostatin (sc-34781), follistatin (sc-30194), TGF-β1 (sc146), phosphorylated-smad3 (sc11769), smad6 (sc13048), smad7 (sc11392), p15 (sc613), p16 (sc1207 and sc1661), p21 (sc756), p27 (sc776), RNAP II (sc899),

Myf5 (sc31946) and goat/rabbit IgG were acquired from Santa Cruz Biotechnologies. Smad3 antibody (06-920) was obtained from Upstate. Fluorophore-conjugated secondary antibodies (Alexa Fluor) were supplied by Invitrogen. HRP-conjugated secondary antibodies were purchased from Santa Cruz Biotechnologies. BrdU labelling reagent was obtained from Sigma. Recombinant human TGF-β1 (RD 240B), recombinant mouse DLL4 (RD 1389) and recombinant mouse myostatin (788-G8-010) were obtained from R&D Systems. TGF-β RI Kinase Inhibitor (50 nM) (#616451) and gamma-Secretase Inhibitor X (50 nM) (#565771) were purchased from Calbiochem. Two × SYBR-Green RT–PCR reaction mixture was purchased from Bio-Rad, and SuperScript One-Step RT–PCR (#10928) from Invitrogen.

**Statistical analysis.** Quantified data are expressed as mean ± s.d. Significance testing was performed using one-way analysis of variance, with an alpha level of 0.01–0.05, to compare data from different experimental groups. A minimum of three replicates were performed for each described experimental condition.

CORRIGENDUM

doi:10.1038/nature19077

# Corrigendum: Imbalance between pSmad3 and Notch induces CDK inhibitors in old muscle stem cells

Morgan E. Carlson, Michael Hsu & Irina M. Conboy

*Nature* **454,** 528–532 (2008); doi:10.1038/nature07034

In Fig. 1a of this Letter, the immunofluorescence images for myostatin and follistatin are inaccurate owing to many versions of this figure in multiple revisions of our manuscript. Specifically, the immunofluorescence panels representing anti-myostatin and anti-follistatin staining were duplicated. We would like to thank the anonymous reader who pointed out this error. We have repeated the age-specific immunofluorescence experiments for myostatin and follistatin, and the results confirm our original conclusion that no age-specific differences are detected (Fig. 1). Furthermore, we have performed quantification of the pixel density, and although there are areas with higher and lower signals for these proteins in both young and old muscle sections, the *P* values suggest no age-specific differences. We thank M. Mehdipour for performing the experiments and analysing the data on age-specific muscle tissue levels of myostatin and follistatin.

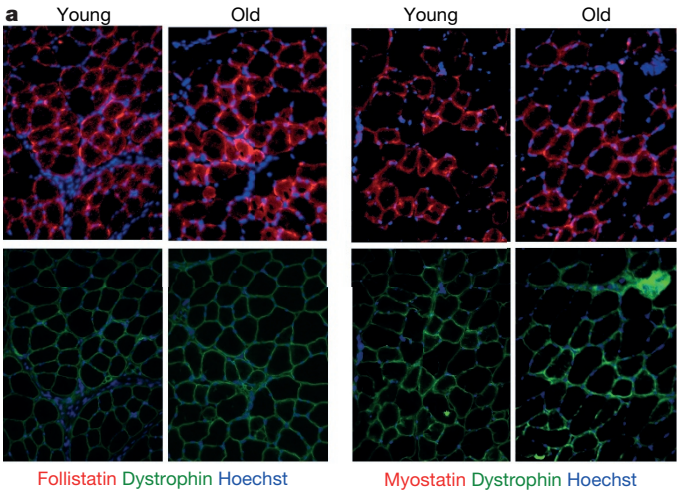


**Figure 1 | This is a repeat of Fig. 1a of the original Letter.** Shown are representative images at ×20. Dystrophin immunofluorescence (green) outlines the muscle fibres in 10-μm skeletal muscle cryosections that are immunostained for follistatin and myostatin (red); Hoechst (blue) stains all nuclei. *P* values for mean pixel density of myostatin and follistatin (with rabbit IgG control signals subtracted) show no statistically significant differences between young and old muscle.